Evaluation of the requirement of an integrated roadmap for identification of lesions in unknown locations using fluorescence-guided surgery in prostate cancer patients.

Authors

Phillipa Meershoek[1], Tessa Buckle[1,2], Matthias N. van Oosterom[1,2], Gijs H. KleinJan[1,2], Henk G. van der Poel[2], Fijs W.B. van Leeuwen[1,2]*

Affiliations

1. Interventional Molecular Imaging Laboratory, Department of Radiology, Leiden University Medical Center, Leiden, the Netherlands.
2. Department of Urology, Netherlands Cancer Center and Antoni van Leeuwenhoek Hospital, Amsterdam, the Netherlands.

*Corresponding author:

Fijs W.B. van Leeuwen

Interventional Molecular Imaging Laboratory

Department of Radiology

Albinusdreef 2, 2300 RC, Leiden

The Netherlands

+31 (0)71-5262042

f.w.b.van_leeuwen@lumc.nl

Keywords

image-guided surgery, prostate cancer, sentinel node biopsy, SPECT/CT, robot-assisted surgery, fluorescence.

Running title

Fluorescence-guidance requires roadmap

ABSTRACT

Rationale: Lymphatic tracers can help visualize the lymphatic drainage patterns and sentinel nodes of individual prostate cancer patients. To determine the role of nuclear medicine in surgical guidance, in particular the positional guidance of a SPECT/CT-based 3D imaging roadmap, in this process we studied to which extend fluorescence-guidance underestimated the number of target lesions.

Methods: SPECT/CT imaging was performed after intraprostatic tracer administration of either ICG-^{99m}Tc-nanocolloid (hybrid tracer group) or ^{99m}Tc-nanocolloid to create a roadmap that depicted all sentinel nodes (SNs). Patients who received ^{99m}Tc-nanocolloid were injected with "free" ICG immediately prior to surgery ("free" ICG group). Before unblinding, fluorescence-guidance was used for intraoperative SN identification. This was followed by extended pelvic lymph node dissection (ePLND). Following unblinding of the SPECT/CT images, the number of missed SN's were recorded and their resection was pursued when there was no risk of intraoperative complications.

Results: Preoperative SPECT/CT revealed no differences in the SN identification rate between ICG-^{99m}Tc-nanocolloid and ^{99m}Tc-nanocolloid. However, fluorescence-guidance only allowed intraoperative removal of all SNs in 40% of patients in the hybrid tracer group and in 20% of patients in the "free" ICG group. Overall, 75.9% of the intraoperatively resected SNs in the hybrid tracer group and 51.8% of the SNs in the "free" ICG group were removed solely under fluorescence-guidance. During ePLND 22 additional SNs were resected (7 in the hybrid tracer group and 15 in the "free" ICG group). After unblinding 18 remaining SNs were identified (6 in the hybrid group and 12 in the "free" ICG group). In the "free" ICG group, ex vivo evaluation of the

excised specimens revealed that 14 SNs removed under ePLND or after unblinding contained radioactivity but no fluorescence.

Conclusions: The preoperative imaging roadmap provided by SPECT/CT enhanced the detection of prostate SNs in more ectopic locations in 17 of the 25 patients and the hybrid tracer ICG-^{99m}Tc-nanocolloid was shown to outperform "free" ICG. Overall, fluorescence-guided pelvic nodal surgery underestimated the number of SNs in 60-80% of patients.

INTRODUCTION

In radioguided surgery, preoperative imaging findings support lesion identification during the intervention. The value that preoperative imaging provides is underlined by the impact that three dimensional (3D) imaging road-maps have had on known radioguidance procedures such as SN resections (SPECT/CT based identification of aberrant tracer uptake) and PSMA-expression targeted resections (PET/CT and SPECT/CT based target definition)(*1-3*). The value of knowing were lesions are located during surgical procedures in relation to the patient's anatomical context is especially eminent when resections are performed in complex anatomies (e.g. the pelvic area).

The success of radioguidance during surgical procedures, fuelled by calls for radioactivity-free alternatives, has sparked the revival of fluorescence-guided surgery (*4*). For instance, the near infra-red (NIR) fluorescent dye Indocyanine green (ICG) has been applied for fluorescence-based lymphangiography in prostate cancer patients (*5,6*). The clinical growth of fluorescence-guided surgery has been further accommodated by the commercial availability of near-infrared fluorescence cameras that depict fluorescence images in anatomical context (*7,8*). Unfortunately, fundamental photophysical limitations such as the tissue attenuation of light limit the use of intraoperative fluorescence-guidance to superficial lesion locations (< 1.0 cm) e.g. surgically exposed tissues (*9,10*). In patients were lesion locations are not accurately defined, this could possibly result in underestimation of the number of lesions.

In an attempt to combine the strengths of radio-and fluorescence- guidance and to overcome the above mentioned limitation of light attenuation, in prostate cancer patients "free" ICG has been used in combination with radioguidance (pre-operative imaging e.g. SPECT/CT and intraoperative gamma tracing) provided by traditional nanocolloids (e.g. ^{99m}Tc-nanocolloid) (*11*).

Limiting in using such a cocktail of tracers is that the individual tracers have different pharmacokinetic properties (*12*), which can yield a mismatch in radioactive and fluorescence findings (*13*). To prevent such a mismatch and to provide fully integrated radio- and fluorescence-guidance towards the identical lesions, bimodal, or rather hybrid, tracers such as ICG-^{99m}Tc-nanocolloid have been introduced (*2,14,15*).

The clinical use of ICG-^{99m}Tc-nanocolloid has in the past allowed us to study the concentration-dependent detection sensitivity of the individual modalities (*14*), but can also be used to determine to which extend fluorescence-guidance underestimates the number of target lesions in a patient. This effect was studied in a blinded randomized controlled trial wherein prostate cancer patients either received ICG-^{99m}Tc-nanocolloid or ^{99m}Tc-nanocolloid and "free" ICG prior to robot assisted SN biopsy and ePLND. SN resection and ePLND were initially performed under fluorescence-guidance alone and the SNs identified on SPECT/CT became available after unblinding. Comparing the outcome of intraoperative fluorescence imaging, ePLND and SPECT/CT guided resections provided insight in the reliability of relying on fluorescence-guidance during surgery.

MATERIALS AND METHODS

Patients

25 patients with histopathologically proven PCa, scheduled for a robot-assisted radical prostatectomy, clinically N0M0 on preoperative imaging, and a risk of nodal metastases of >5% according to the Briganti nomogram were included (*16*). Patients participating in a clinical trial comparing two methods of multimodal sentinel node tracing were asked to participate in the sub

study on the value of preoperative SPECT/CT (M13PSN). Patients were randomly allocated to receive either a preoperative injection into the prostate with the hybrid tracer, ICG-^{99m}Tc-nanocolloid (hybrid tracer group; 15 patients) or a preoperative injection with ^{99m}Tc-nanocolloid followed by an intraoperative injection of "free" ICG (further noted as "free" ICG group; 10 patients). Exclusion criteria were a history of iodine allergy, hyperthyroid or thyroidal adenoma, kidney insufficiency, surgical inaccessibility or incorrect implementation of the procedure.

All procedures performed in this study were in accordance with the 1964 Helsinki declaration and its later amendments or comparable ethical standards and after approval was obtained by the local ethics committee of The Netherlands Cancer Institute - Antoni van Leeuwenhoek Hospital (NL46580.031.13). Written informed consent was obtained from all patients prior to inclusion in this study.

Tracer administration and preoperative imaging

The radioisotopes (500 μg human serum albumin in 2ml) were injected either as hybrid tracer (ICG-^{99m}Tc-nanocolloid) or as monomodal tracer (^{99m}Tc-nanocolloid) with a second injection of free ICG into the prostate minutes before the lymph node dissection. ICG-^{99m}Tc-nanocolloid contained 0,25 mg ICG (total volume), while a "free" ICG injection meant 5 mg of ICG was administered (20-fold more) to the patient also constituting a two-fold increase in injected volume (4ml total). No difference in the amount of radioactivity used could be detected between both groups (administered dose of 205.1 ± 17.4 MBq and 207.0 ± 15.3 MBq, respectively, p=0.793).

Following radiotracer administration, lymphatic mapping including SPECT/CT was performed as previously described (*15,17*). Based on the reproducibility in the lymphatic drainage of ^{99m}Tc-nanocolloid and ICG-^{99m}Tc-nanocolloid (*17*), in both groups SNs identified on SPECT/CT were considered to be the golden standard.

Patients In the "free" ICG group received an additional four transrectal intraprostatic injections of ICG at five-ten minutes prior to initiating the procedure, while under full anesthesia.

Surgical procedure

Approximately four hours after the preoperative injection of the hybrid or radioactive tracers, patients were transferred to the operation room. All procedures were performed by two experienced robotic surgeons using a da Vinci Si surgical system (Intuitive surgical, Sunnyvale, CA, US). Initially, the operating surgeon was blinded for the SPECT/CT imaging data and pursued the SNs intraoperatively with near-infrared (NIR) fluorescence imaging only. This was done using the ICG-tuned Firefly camera integrated in the da Vinci Si surgical system. Fluorescence-based SN resection was followed by resection of the extended pelvic lymph node template (ePLND) (obturator fossa, external iliac vessels, both up to the ureter-vessel crossing on both sides). To identify ^{99m}Tc and ICG containing nodes *ex vivo,* additional measurements were performed on the surgical specimens using a modified Photodynamic Eye (PDE-mod) NIR fluorescence camera system (Hamamatsu Photonics, Japan (*7*)) and gamma probe (Neoprobe, Johnson & Johnson Medical, Hamburg, Germany). SNs removed in the ePLND template but not primarily detected by fluorescence-guidance intraoperatively were labelled SN when containing an ex vivo gamma signal above background.

Subsequently the surgeon was unblinded for the preoperative SPECT/CT images. These images were then consulted to confirm removal of all SNs under fluorescence-guidance and or during ePLND. SNs that were missed were pursued based on the positional guidance of SPECT/CT. *In vivo* detection using an intraoperative gamma-probe was only used after unblinding. Excised specimens were evaluated *ex vivo* to validate their fluorescent and radioactive content.

Quantification lesion underestimation under fluorescence-guidance

The included the number and location of the SNs identified using fluorescence-guidance alone, both within and outside the ePLND template were noted for the two groups. After unblinding, the number and location of the intraoperatively identified SNs were compared to the number and location of SNs identified on preoperative imaging. Correlation between the radioactive and fluorescent content of the excised specimens was included to identify SNs that were radioactive but not fluorescent.

Pathology

The excised lymph nodes were pathologically examined for the presence of macro/micro-metastases and/or isolated tumor cells, according to previously described protocols (*8,18*). The resected prostatectomy specimens were examined and classified for pathologic tumor stage (*8*).

Complications

Intraoperative and postoperative complications were scored. Postoperative complications were included when occurred within 90 days after surgery and were divided according to the Clavien Dindo (CD) score.

Follow up

Biochemical recurrence was defined as a PSA level ≥0.2 ng/ml after prostatectomy and ePLND. Patients were screened (watch-and-wait principle) for biochemical recurrence every 6 months postoperatively for up to 57 months post-surgery. No adjuvant radiotherapy or androgen ablation therapy was used in the absence of biochemical recurrence. When PSA levels over 0.2 ng/ml were detected after prostatectomy, ^{68}Ga-PSMA-PET imaging was performed to detect the location of disease recurrence.

Statistics

Statistical analysis was performed using SPSS version 22 (IBM). Chi-square and Fisher's Exact tests were used for comparison of distributions in patient characteristics. Endpoint of the study was the number of patients with missed SN apparent upon unblinding of the SPECT/CT imaging. Use of the hybrid tracer was considered necessary when in at least one of 25 men additional nodes were found after unblinding.

RESULTS

Patients

Patient characteristics are summarized in Table 1. All patients had clinically Gleason score 7 or higher cancer prior to surgery and clinical stages ranged between cT1c and cT3b and a mean Briganti risk score for nodal metastases of 16.6% (13%). No significant differences were seen between patients in the hybrid tracer or "free" ICG group.

Preoperative imaging findings

In total 111 SNs were identified on preoperative SPECT/CT (Table 2), with a mean number of 4.4 $\pm$ 2.5 SNs identified per patient in the complete patient group. Of these SNs, 57 (3.8 $\pm$ 1.8 per patient) were found in the hybrid tracer group and 54 (5.4 $\pm$ 3.0 per patient) were found in the "free" ICG group. Of the 82 SNs identified within the eLNPD template, 50 SNs were found in the hybrid tracer group (87.7% of SNs within this group) and 32 SNs (59.3% of SNs within this group) were found in the "free" ICG group. Overall, the most prevalent nodal location was the obturator fossa (31.5% of all SNs; Table 1).

Intraoperative findings

Intraoperatively, the hybrid tracer group allowed the visualization of the exact same lesions identified on preoperative SPECT, while literature indicates there could be discrepancy between the SN's detected with ^{99m}Tc-nanocolloid and "free" ICG (*13*). A total of 114 SNs were resected

(Table 2, Figure 1). The fact that fluorescence imaging was able to discriminate between cluster nodes that are visual as one hotspot on SPECT/CT, helps explain why the number was slightly higher than the SN's defined at preoperative imaging (*19*). In eight patients (6/15 (40%) in the hybrid tracer group and 2/10 (20%) in the "free" ICG group) all SNs could be removed under fluorescence-guidance alone. In the remaining 17 patients one or more SNs were missed. Overall, 75.9% of the SNs in the hybrid tracer group (44/58) were removed under fluorescence-guidance, compared to 51.8% (29/56) in the "free" ICG group (Table 2). In addition, in the "free" ICG group 24% more fluorescent nonSNs were removed compared to the hybrid tracer group (13 nonSNs (62%) vs. 8 nonSNs (38%), respectively).

Of the 58 fluorescent SNs found in the hybrid tracer group, 75.9% (44 SNs) was located within the ePLND template (Table 2, Figure 1). In agreement with the preoperative findings, only 51.8% (29 SNs) of the 56 fluorescent SNs in the "free" ICG group were located within the ePLND template. This finding underlines the difference in drainage kinetic between "free" ICG and radiocolloids (*12*).

After unblinding of the SPECT/CT images to the surgeon, 18 SNs (in 11 patients) were identified that were not yet resected (6 SNs (10.3%) in the hybrid tracer group and 12 SNs (21.4%) in the "free" ICG group; Table 2, Figure 1). Of these initially missed SNs only one was located within the ePLND template (external iliac region; Figure 2), the remaining nodes were located outside the ePLND template (Table 2). To avoid damage to healthy tissue, only the SN located within the ePLND template was surgically removed.

Ex vivo evaluation of the radioactive and fluorescent content of the excised specimens revealed that of the 27 SNs that were removed under ePLND or after unblinding of the

preoperative SPECT images in the "free" ICG group, 14 SNs (in 7/10 (70%) of patients) contained radioactivity but no fluorescence (Table 2, Figure 1). This mismatch was not seen in the hybrid tracer group.

Pathology

Pathological analysis yielded non-radical resection margins after prostatectomy in eight patients and LN metastases in six patients (24%; Table 2). Of the 13 metastases found, ten were identified in nodes specified as SN on preoperative imaging. 9 of these SNs were found in the hybrid tracer group and one was found in the "free" ICG group (Figure 1). In 4 patients (66.7%) more than one (2-4) positive node was found. In three of these patients' additional metastases were found in non-SN nodes (1/patient). In one patient in the "free" ICG group a false-negative but tumor positive SN was found in the ePLND specimens but was missed on SPECT/CT; the preoperatively specified SNs and fluorescent nodes in this patient were all tumor negative. Although displaying 1600 counts with the gamma probe *ex vivo*, this SN was not classified as SNs on preoperative imaging. This finding indicates that in some cases (1/111 SNs; 1%) the sensitivity of SPECT/CT may limit nodal identification.

Complications

The overall complication rate within 90 days after surgery was 16.0%, which is in line with previously reported complication rates (*20*). No intraoperative complications were recorded and no substantial difference in postsurgical complications was seen between the hybrid tracer group and the "free" ICG group; in the hybrid tracer group, one CD type 2 (pulmonary embolism) and

one CD type 3b (cicatricial port site hernia) were registered. In the "free" ICG group, one CD type 1 (incontinence) and one CD type 2 (urinary tract infection) complication were recorded.

Follow up

Mean follow-up of 23.3 months (range 7-57 months) was available for 23 patients (13 in the hybrid tracer group and 10 in the "free" ICG group). Of the patients with follow-up <12 months (N=10), 90% had PSA levels <0.01ng/mL. No differences in biochemical recurrences were seen between the hybrid tracer group and the "free" ICG group.

Of the eight patients wherein resection margins were deemed to be non-radical at pathology, four had PSA levels <0.01ng/mL (mean follow-up 7.2 months, range 7-8 months) and four had PSA levels between 0.03 and 7.56 ng/mL (mean follow-up 49 months, range 48-50 months). Three of the four patients with a biochemical recurrence had nodal metastasis. All four underwent additional radiotherapy. One patient (PSA <0.01 ng/mL) died of lung carcinoma within a year after prostate cancer surgery.

The six patients wherein lymph node metastases were found were subjected to watch and wait follow-up (mean follow-up 47,7 months, range to date 33-57 months). Four were received additional therapies after surgery (radiotherapy (N=4) and further LN dissection of the pelvis (N=1)), additional chemotherapy (N=2) after a rise in PSA level and subsequent ^{68}Ga-PSMA PET imaging.

DISCUSSION

As procedural cost savings would warrant simplification of image-guided surgery approaches, insight in the value of fluorescence-guidance and omission of the use of relatively costly roadmaps based on preoperative imaging findings is in demand. By demonstrating that blinding surgeons to SPECT/CT data means that the number of SNs is underestimated using fluorescence-guidance alone, our study helps understand to what extend light-attenuation influences the process of image-guided surgery.

Conform a previous reproducibility study by Brouwer et al, no difference in the overall preoperative SN identification rate (radioactivity based) was seen between ICG-^{99m}Tc-nanocolloid and ^{99m}Tc-nanocolloid (17). To our surprize, the two groups - although patient selection was identical and patient inclusion was blinded- yielded different numbers of SN's identified beyond the ePLND template by SPECT/CT. When comparing the intraoperative SN identification rate of ICG-^{99m}Tc-nanocolloid and "free" ICG (fluorescence-based), clear differences were seen; 24.1% of SNs the hybrid tracer group and 49.2% of SNs in the "free" ICG group were missed when resection was pursued with fluorescence-guidance alone. Moreover, ex vivo assessment of excised specimens in the "free" ICG group revealed a mismatch between radioactive and fluorescent content in the SNs in 70% of patients. The latter indicates a discrepancy in the distribution pattern between ^{99m}Tc-nanocolloid and "free" ICG and couches the arguments behind using a hybrid tracer for image-guidance rather than rely on a combination of a radio and fluorescent tracers. Important to note is that while the 20-times higher dose of ICG in the "free" ICG group did not lead to increased intensities that subsequently led to better *in vivo* SN identification, rather a

substantial higher number (24%) of fluorescent nonSNs were stained and removed in the free"

ICG group. These nonSNs could be considered as false positives.

The findings presented here indicate that, similar to what is reported for radioguided

surgery (*2,7,21*), the accuracy of fluorescence-guided surgery towards lesions in unknown

locations is related to the availability of accurate surgical roadmaps in the form of preoperative

imaging data. This not only supports the concept of using hybrid tracers for surgical guidance (*22*),

it also strengthens the suggested use of intraoperative augmented- and virtual-reality-based

navigation to improve the position fluorescence camera's relative to the lesion location (*23*).

In prostate cancer, lymphatic metastases often occur in unexpected locations (*24*). In line

with these reports, a substantial amount of SNs were found outside the ePLND template (17/73

SNs (23.3%) in 8/25 patients (32%)). The fact that fluorescence-guidance structurally misses

lesions in unexpected locations, would mean that receptor-targeted fluorescence-guided surgery

procedures performed without accompanying preoperative imaging data could translate to a

poor oncological outcome. Assuming that the use of tracers in image-guided surgery procedures

has the purpose to enable radical surgical excision of lesions, this paints an alarming picture for

the future of the field. Follow-up data of large randomized studies wherein tumour-specific

tracers are applied will be needed to confirm if this is indeed the case. Given the superior

detection sensitivity of radiotracers, this potential risk can be easily mitigated through the

implementation of corresponding preoperative imaging data through the use of hybrid tracers,

an exponentially growing field of research. Current efforts in hybrid tracer developments include

e.g. Cerenkov imaging (*25*) small molecules (*26*) peptides (*27*), mAbs (*28*) and nanoparticles (*29*).

One of the strengths of this study was the possibility to remove the SN's that were missed under fluorescence-guidance alone after unblinding the surgeon by using the preoperative SPECT images. The additional value of SPECT/CT imaging was evident despite the small sample size and was relevant for both tracer formulations, strengthening the observation. However, this set-up does not allow evaluation of the complication rate and/or possible differences in follow-up based solely on intraoperative fluorescence-guidance results. Also the small sample size complicates a head-to-head comparison of the two different tracer formulations used. The latter is currently being addressed in a follow-up study with a larger sample size.

In prostate cancer the SN procedure is applied to identify micrometastases and in doing so the procedure positively impacts recurrence values. Recently this concept proved to be of value in PSMA-PET negative patients (*30*). As not all SNs will contain metastases, the operating surgeon always has to balance the benefit of their resection to the potential harm that may be caused to the patient (e.g. lymphedema, thromboembolic evens, ureteral injury and neurovascular injuries). In this case that meant that some SNs (14.9%) were not surgically resected. Compared to indications wherein receptor-targeted tracers would have been relied upon for surgical-guidance, using SN procedures to study the accuracy of fluorescence-guidance only limits the negative impact that miss-rates could have had on the final patient outcome.

CONCLUSIONS

Intraoperative comparison between the hybrid tracer ICG-^{99m}Tc-nanocolloid and "free" ICG revealed that accurate surgical-guidance to ectopic SNs could not be achieved when solely relying

on fluorescence-guidance in 17 of the 25 patients included in this study. The preoperative imaging roadmap provided by SPECT/CT enhanced the detection of prostate SNs in more ectopic locations and the hybrid tracer ICG-^{99m}Tc-nanocolloid was shown to outperform "free" ICG.

Conflict of interest statement:

No potential conflicts of interest relevant to this article exist.

KEY POINTS:

QUESTION: Can fluorescence-guided surgery help identify all lesions in unknown locations or is the integrated use of a roadmap created by preoperative imaging mandatory?

PERTINENT FINDINGS: In a cohort study evaluating the extent to which fluorescence-guidance underestimated the number of target lesions in twenty-five prostate cancer patients the preoperative imaging roadmap provided by SPECT/CT was shown to enhance the detection of prostate SNs in more ectopic locations. Use of the hybrid tracer ICG-^{99m}Tc-nanocolloid was shown to outperform "free" ICG.

IMPLICATIONS FOR PATIENT CARE: Meaning accurate surgical-guidance to ectopic SNs benefits from a hybrid approach wherein fluorescence-guidance is complemented by a preoperative imaging roadmap provided by SPECT/CT.

REFERENCES

1. Robu S, Schottelius M, Eiber M, et al. Preclinical Evaluation and First Patient Application of 99mTc-PSMA-I&S for SPECT Imaging and Radioguided Surgery in Prostate Cancer. *J Nucl Med.* 2017;58:235-242.

2. van Leeuwen FWB, Winter A, van Der Poel HG, et al. Technologies for image-guided surgery for managing lymphatic metastases in prostate cancer. *Nat Rev Urol.* 2019;16:159-171.

3. Vermeeren L, van der Ploeg IM, Olmos RA, et al. SPECT/CT for preoperative sentinel node localization. *J Surg Oncol.* 2010;101:184-190.

4. van Leeuwen FW, Hardwick JC, van Erkel AR. Luminescence-based Imaging Approaches in the Field of Interventional Molecular Imaging. *Radiology.* 2015;276:12-29.

5. Manny TB, Patel M, Hemal AK. Fluorescence-enhanced robotic radical prostatectomy using real-time lymphangiography and tissue marking with percutaneous injection of unconjugated indocyanine green: the initial clinical experience in 50 patients. *Eur Urol.* 2014;65:1162-1168.

6. Wit EM, Acar C, Grivas N, et al. Sentinel Node Procedure in Prostate Cancer: A Systematic Review to Assess Diagnostic Accuracy. *Eur Urol.* 2017;71:596-605.

7. van den Berg NS, Miwa M, KleinJan GH, et al. (Near-Infrared) Fluorescence-Guided Surgery Under Ambient Light Conditions: A Next Step to Embedment of the Technology in Clinical Routine. *Ann Surg Oncol.* 2016;23:2586-2595.

8. KleinJan GH, van den Berg NS, Brouwer OR, et al. Optimisation of fluorescence guidance during robot-assisted laparoscopic sentinel node biopsy for prostate cancer. *Eur Urol.* 2014;66:991-998.

9. Stammes MA, Bugby SL, Porta T, et al. Modalities for image- and molecular-guided cancer surgery. *Br J Surg.* 2018;105:e69-e83.

10. Teraphongphom N, Kong CS, Warram JM, Rosenthal EL. Specimen mapping in head and neck cancer using fluorescence imaging. *Laryngoscope Investig Otolaryngol.* 2017;2:447-452.

11. Jeschke S, Lusuardi L, Myatt A, et al. Visualisation of the lymph node pathway in real time by laparoscopic radioisotope- and fluorescence-guided sentinel lymph node dissection in prostate cancer staging. *Urology.* 2012;80:1080-1086.

12. Van Den Berg NS, Buckle T, Kleinjan GI, et al. Hybrid tracers for sentinel node biopsy. *Q J Nucl Med Mol Imaging.* 2014;58:193-206.

13. Soergel P, Kirschke J, Klapdor R, et al. Sentinel lymphadenectomy in cervical cancer using near infrared fluorescence from indocyanine green combined with technetium-99m-nanocolloid. *Lasers Surg Med.* 2018;50:994-1001.

14. KleinJan GH, Bunschoten A, van den Berg NS, et al. Fluorescence guided surgery and tracer-dose, fact or fiction? *Eur J Nucl Med Mol Imaging.* 2016;43:1857-1867.

15. van der Poel HG, Buckle T, Brouwer OR, Valdes Olmos RA, van Leeuwen FW. Intraoperative laparoscopic fluorescence guidance to the sentinel lymph node in prostate cancer patients: clinical proof of concept of an integrated functional imaging approach using a multimodal tracer. *Eur Urol.* 2011;60:826-833.

16. Briganti A, Larcher A, Abdollah F, et al. Updated nomogram predicting lymph node invasion in patients with prostate cancer undergoing extended pelvic lymph node dissection: the essential importance of percentage of positive cores. *Eur Urol.* 2012;61:480-487.

17.   Brouwer OR, Buckle T, Vermeeren L, et al. Comparing the hybrid fluorescent-radioactive tracer indocyanine green-99mTc-nanocolloid with 99mTc-nanocolloid for sentinel node identification: a validation study using lymphoscintigraphy and SPECT/CT. *J Nucl Med.* 2012;53:1034-1040.

18.   KleinJan GH, van den Berg NS, de Jong J, et al. Multimodal hybrid imaging agents for sentinel node mapping as a means to (re)connect nuclear medicine to advances made in robot-assisted surgery. *Eur J Nucl Med Mol Imaging.* 2016;43:1278-1287.

19.   KleinJan GH, van Werkhoven E, van den Berg NS, et al. The best of both worlds: a hybrid approach for optimal pre- and intraoperative identification of sentinel lymph nodes. *Eur J Nucl Med Mol Imaging.* 2018;45:1915-1925.

20.   Liss MA, Palazzi K, Stroup SP, et al. Outcomes and complications of pelvic lymph node dissection during robotic-assisted radical prostatectomy. *World J Urol.* 2013;31:481-488.

21.   van Leeuwen FW, Valdes-Olmos R, Buckle T, Vidal-Sicart S. Hybrid surgical guidance based on the integration of radionuclear and optical technologies. *Br J Radiol.* 2016;89:20150797.

22.   Bugby SL, Lees JE, Perkins AC. Hybrid intraoperative imaging techniques in radioguided surgery: present clinical applications and future outlook. *Clin Transl Imaging.* 2017;5:323-341.

23.   van Oosterom MN, Rietbergen DDD, Welling MM, et al. Recent advances in nuclear and hybrid detection modalities for image-guided surgery. *Expert Rev Med Devices.* 2019.

24.   Van den Bergh L, Joniau S, Haustermans K, et al. Reliability of sentinel node procedure for lymph node staging in prostate cancer patients at high risk for lymph node involvement. *Acta Oncol.* 2015;54:896-902.

25.   Tamura R, Pratt EC, Grimm J. Innovations in Nuclear Imaging Instrumentation: Cerenkov Imaging. *Semin Nucl Med.* 2018;48:359-366.

26.   Hensbergen AWB, Buckle T, van Willigen DM, Schottelius M, Welling MM, van der Wijk FA, Maurer T, van der Poel HG, van der Pluijm, G, van Weerden WM, Wester H-J, van Leeuwen FWB. Hybrid Tracers Based on Cyanine Backbones Targeting Prostate-Specific Membrane Antigen – Tuning Pharmacokinetic Properties and Exploring Dye–Protein Interaction *J Nucl Med.* 2019;Epub ahead of print September 3, 2019.

27.   Kuil J, Velders AH, van Leeuwen FW. Multimodal tumor-targeting peptides functionalized with both a radio- and a fluorescent label. *Bioconjug Chem.* 2010;21:1709-1719.

28.   Lutje S, Heskamp S, Franssen GM, et al. Development and characterization of a theranostic multimodal anti-PSMA targeting agent for imaging, surgical guidance, and targeted photodynamic therapy of PSMA-expressing tumors. *Theranostics.* 2019;9:2924-2938.

29.   Smith BR, Gambhir SS. Nanomaterials for In Vivo Imaging. *Chem Rev.* 2017;117:901-986.

30.   Hinsenveld FJW, EMK Wit, van Leeuwen PJ, Brouwer OR, Donswijk,M.L, Tillier CN, Vegt, E, van Muilekom HAM, van Oosterom MN, van Leeuwen FWB, van der Poel HG. Prostate-specific membrane antigen positron emission tomography/computed tomography combined with sentinel node biopsy for primary lymph node staging in prostate cancer *J Nucl Med.* 2019;Epub ahead of print.

Tables and Figures

Table 1: Patient characteristics

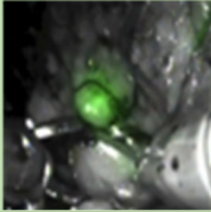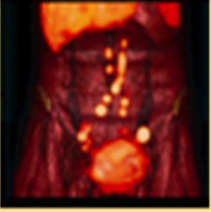|	All patients N= 25	Hybrid tracer group N= 15	"Free" ICG group N= 10	P-value
Age (years) at surgery mean (SD)	65.4 (6.1)	64.3 (8.4)	67.4 (4.4)	0.247
PSA (ng/ml) at diagnosis mean (SD)	8.6 (3.9)	9.1 (4.6)	7.7 (2.3)	0.383
range	2.7 – 22.5	2.7 – 22.5	4.31 – 12.04	
Clinical stage				0.870
- cT1c	5	4	1	
- cT2a	4	2	2	
- cT2b	3	1	2	
- cT2c	7	4	3	
- cT3a	5	3	2	
- cT3b	1	1	0	
Biopsy Gleason sum				1.000
- 6	2	1	1	
- 7	17	10	7	
- 8	3	2	1	
- 9	3	2	1	
Prostate volume mean (SD) (ml)	50.2 (21)	48.1 (20.0)	52.4 (25.8)	0.641
Briganti score mean (SD)	16.6 % (16.1)	16.6 (15.6)	16.6 (17.8)	0.996
Pathological stage				0.596
- pT2a	4	1	3	
- pT2c	14	9	5	
- pT3a	5	3	2	
- pT3b	1	1	0	
- pT4	1	1	0	
Pathological Gleason sum				0.194
- 6	3	3	0	
- 7	15	7	8	
- 8	3	3	0	
- 9	2	2	2	
Nodal status				1.00
- pN0	19	11	8	
- pN1	6	4	2	

N = number; SD = standard deviation

Table 2: Results identified and removed SNs and LNs

	All patients (N=25)	Hybrid tracer group (N=15)	"Free" ICG group (N=10)
SPECT/CT			
Total number of identified SN	111	57	54
Mean no. SNs per patient (SD)	4.4 (2.5)	3.8 (1.8)	5.4 (3.0)
SNs *inside ePLND template*	82 (73.9%)	50 (87.7%)	32 (59.3%)
- External iliac	26	16	10
- Internal iliac	21	13	8
- Obturator fossa	35	21	14
SNs *outside ePLND template*	29 (26.1%)	7 (12.3%)	22 (40.7%)
- Common iliac	12	4	8
- Paravesical	3	3	0
- Presacral	5	0	5
- Pararectal	6	0	6
- Inguinal	3	0	3
Surgery			
Total No. of resected SNs	114	58	56
Total No. of SNs removed under fluorescence-guidance	73 (64.0%)	44 (75.9%)	29 (51.8%)
No. SNs per patient (SD)	4.6 (3.0)	3.8 (2.0)	5.6 (3.8)
Fluorescent SNs removed *inside ePLND template*	56 (79.5%)	34 (77.3%)	22 (75.9%)
- Externa iliac	20	12	8
- Internal iliac	11	7	4
- Obturator fossa	25	15	10
Fluorescent SNs removed *outside ePLND template*	17 (23.3%)	10 (29.4%)	7 (24.1%)
- Common iliac	2	2	0
- Marcille	0	0	0
- Cloquet	0	0	0
- Pararectal	5	0	5
- Presacral	2	0	2
- Umbilical ligament	8	8	0
- Aorta bifurcation	0	0	0
- Undefined	0	0	0
No. SNs resected during eLNPD	22 (19.3%)	7 (12.1%)	15 (26.8%)
No. of SNs identified after unblinding of SPECT	18 (15.8%)	6 (10.3%)	12 (21.4%)
No. of SNs removed after unblinding	1	-	1

No. of SNs not removed after unblinding *Location*: Inside ePLND template - Internal iliac Outside ePLND template - Common iliac - Pararectal - Inguinal	17 3 4 8 2	7 2 3 2 -	10 1 1 6 2
Total No. of non-SNs removed under fluorescence-guidance	21	8	13
Ex vivo imaging			
No. of SNs that were fluorescent but not radioactive	14	0	14
No. of patients	7 (28%)	0 (0%)	7 (70%)
Pathology			
No. of tumor positive SNs (no. of patients)	10 (6)	9 (4)	1 (1)
No. of non-SNs removed	320	177	143
No. of tumor positive nodes in non-SNs (no. of patients)	3 (3)	2 (2)	1 (1)
Tumor positive nodes *inside ePLND template* - Externa iliac - Internal iliac - Obturator fossa Tumor positive nodes *outside ePLND template* - Marcille - Cloquet - Pararectal	 5 2 3 1 1 1	 5** 2 2 1 1	 1* 1

** = 2x non-SN, * = 1x non-SN

Figure 1. Overview intraoperative SN removal and tumor positive SNs. Hybrid = hybrid tracer group and ICG = "free" ICG group.
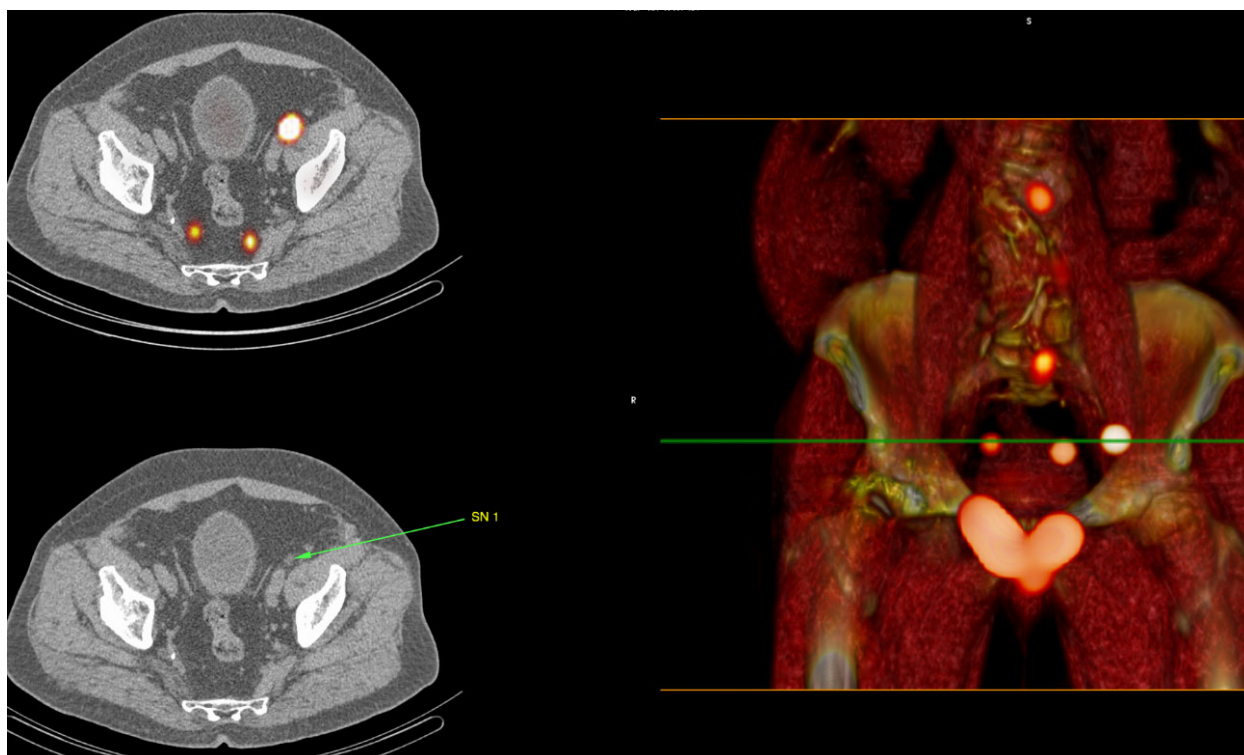
Figure 2. Location Iliacal SN resected after unblinding the surgeon to the SPECT/CT.